

University of Groningen

Measurement of the ratio of branching fractions and difference in CP asymmetries of the decays $B^+ \rightarrow J/\psi \pi^+$ and $B^+ \rightarrow J/\psi K^+$

LHCb Collaboration

Published in:
Journal of High Energy Physics

DOI:
[10.1007/JHEP03\(2017\)036](https://doi.org/10.1007/JHEP03(2017)036)

IMPORTANT NOTE: You are advised to consult the publisher's version (publisher's PDF) if you wish to cite from it. Please check the document version below.

Document Version
Publisher's PDF, also known as Version of record

Publication date:
2017

[Link to publication in University of Groningen/UMCG research database](#)

Citation for published version (APA):

LHCb Collaboration (2017). Measurement of the ratio of branching fractions and difference in CP asymmetries of the decays $B^+ \rightarrow J/\psi \pi^+$ and $B^+ \rightarrow J/\psi K^+$. *Journal of High Energy Physics*, 2017(3), [036]. [https://doi.org/10.1007/JHEP03\(2017\)036](https://doi.org/10.1007/JHEP03(2017)036)

Copyright

Other than for strictly personal use, it is not permitted to download or to forward/distribute the text or part of it without the consent of the author(s) and/or copyright holder(s), unless the work is under an open content license (like Creative Commons).

The publication may also be distributed here under the terms of Article 25fa of the Dutch Copyright Act, indicated by the "Taverne" license. More information can be found on the University of Groningen website: <https://www.rug.nl/library/open-access/self-archiving-pure/taverne-amendment>.

Take-down policy

If you believe that this document breaches copyright please contact us providing details, and we will remove access to the work immediately and investigate your claim.

Downloaded from the University of Groningen/UMCG research database (Pure): <http://www.rug.nl/research/portal>. For technical reasons the number of authors shown on this cover page is limited to 10 maximum.

Measurement of the ratio of branching fractions and difference in CP asymmetries of the decays

$$B^+ \rightarrow J/\psi\pi^+ \text{ and } B^+ \rightarrow J/\psi K^+$$



The LHCb collaboration

E-mail: xuhao.yuan@cern.ch

ABSTRACT: The ratio of branching fractions and the difference in CP asymmetries of the decays $B^+ \rightarrow J/\psi\pi^+$ and $B^+ \rightarrow J/\psi K^+$ are measured using a data sample of pp collisions collected by the LHCb experiment, corresponding to an integrated luminosity of 3 fb^{-1} at centre-of-mass energies of 7 and 8 TeV. The results are

$$\frac{\mathcal{B}(B^+ \rightarrow J/\psi\pi^+)}{\mathcal{B}(B^+ \rightarrow J/\psi K^+)} = (3.83 \pm 0.03 \pm 0.03) \times 10^{-2},$$

$$\mathcal{A}^{\text{CP}}(B^+ \rightarrow J/\psi\pi^+) - \mathcal{A}^{\text{CP}}(B^+ \rightarrow J/\psi K^+) = (1.82 \pm 0.86 \pm 0.14) \times 10^{-2},$$

where the first uncertainties are statistical and the second are systematic. Combining this result with a recent LHCb measurement of $\mathcal{A}^{\text{CP}}(B^+ \rightarrow J/\psi K^+)$ provides the most precise estimate to date of CP violation in the decay $B^+ \rightarrow J/\psi\pi^+$,

$$\mathcal{A}^{\text{CP}}(B^+ \rightarrow J/\psi\pi^+) = (1.91 \pm 0.89 \pm 0.16) \times 10^{-2}.$$

KEYWORDS: B physics, Branching fraction, CP violation, Hadron-Hadron scattering (experiments)

ARXIV EPRINT: [1612.06116](https://arxiv.org/abs/1612.06116)

Contents

1	Introduction	1
2	Detector and simulation	2
3	Event selection	3
4	Signal yield determination	4
5	Efficiency corrections	5
6	Systematic uncertainties	7
7	Results and conclusion	9
	The LHCb collaboration	13

1 Introduction

In the Standard Model, the decay $B^+ \rightarrow J/\psi K^+$ proceeds via a $b \rightarrow c\bar{c}s$ quark transition¹ and, since this process is dominated by a Cabibbo-favoured tree diagram, it is expected to exhibit negligible CP violation [1]. By contrast, for the decay $B^+ \rightarrow J/\psi \pi^+$, which proceeds via $b \rightarrow c\bar{c}d$, CP violation up to the percent level can be generated by interference between the suppressed tree-level diagram and additional gluonic penguin (loop) diagrams as shown in figure 1. Measurements of the branching fraction and CP asymmetry of the decay $B^+ \rightarrow J/\psi \pi^+$ can provide information about the size of the penguin-diagram contributions relative to that of the tree diagram. This is critical for estimating the effects of penguin-diagram contributions in $b \rightarrow c\bar{c}s$ decays on the determination of the CP violation parameter $\sin 2\beta$ [2, 3].

The world average of the branching fraction $\mathcal{B}(B^+ \rightarrow J/\psi \pi^+)$ is $(4.1 \pm 0.4) \times 10^{-4}$ [4], with no significant CP asymmetry observed so far. The world average value of $\mathcal{A}^{CP}(B^+ \rightarrow J/\psi \pi^+)$, which includes measurements from Belle, BaBar, D0 and LHCb [5–8], is $(1.0 \pm 2.8) \times 10^{-2}$ [4].

In an earlier analysis of a sample of pp collision data corresponding to an integrated luminosity of 0.37 fb^{-1} [8], LHCb measured the CP asymmetry $\mathcal{A}^{CP}(B^+ \rightarrow J/\psi \pi^+) = (0.5 \pm 2.7 \pm 1.1) \times 10^{-2}$, as well as the ratio of branching fractions

$$\mathcal{R}_{\pi/K} \equiv \frac{\mathcal{B}(B^+ \rightarrow J/\psi \pi^+)}{\mathcal{B}(B^+ \rightarrow J/\psi K^+)} = (3.83 \pm 0.11 \pm 0.07) \times 10^{-2}. \quad (1.1)$$

¹Unless otherwise specified, the inclusion of charge-conjugate processes is implied throughout this paper.

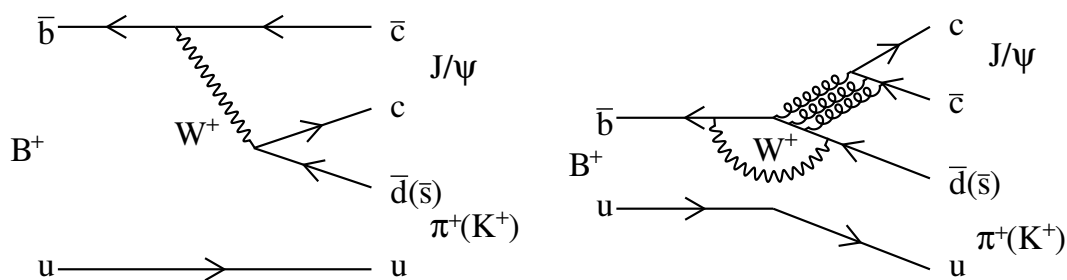


Figure 1. Feynman diagrams for $B^+ \rightarrow J/\psi \pi^+(K^+)$ decays at the tree (left) and one-loop (right) levels.

This paper reports an update of the analysis and uses the full pp data sample from the LHC Run 1, corresponding to 1 fb^{-1} collected at a centre-of-mass energy of 7 TeV and 2 fb^{-1} at 8 TeV , and measures $\mathcal{R}_{\pi/K}$ and $\Delta\mathcal{A}^{\text{CP}} \equiv \mathcal{A}^{\text{CP}}(B^+ \rightarrow J/\psi \pi^+) - \mathcal{A}^{\text{CP}}(B^+ \rightarrow J/\psi K^+)$, where these two decays are reconstructed using the dimuon decay mode of the J/ψ meson. The result for $\Delta\mathcal{A}^{\text{CP}}$ is combined with the $\mathcal{A}^{\text{CP}}(B^+ \rightarrow J/\psi K^+)$ measurement from another LHCb analysis [9] to obtain $\mathcal{A}^{\text{CP}}(B^+ \rightarrow J/\psi \pi^+)$.

2 Detector and simulation

The LHCb detector [10, 11] is a single-arm forward spectrometer covering the pseudorapidity range $2 < \eta < 5$, designed for the study of particles containing b or c quarks. The detector includes a high-precision tracking system consisting of a silicon-strip vertex detector surrounding the pp interaction region, a large-area silicon-strip detector located upstream of a dipole magnet with a bending power of about 4 Tm , and three stations of silicon-strip detectors and straw drift tubes placed downstream of the magnet. The tracking system provides a measurement of momentum, p , of charged particles with a relative uncertainty that varies from 0.5% at low momentum to 1.0% at $200 \text{ GeV}/c$. The minimum distance of a track to a primary vertex (PV), the impact parameter, is measured with a resolution of $(15 + 29/p_T) \mu\text{m}$, where p_T is the component of the momentum transverse to the beam, in GeV/c . Different types of charged hadrons are distinguished using information from two ring-imaging Cherenkov detectors. Photons, electrons and hadrons are identified by a calorimeter system consisting of scintillating-pad and preshower detectors, an electromagnetic calorimeter and a hadronic calorimeter. Muons are identified by a system composed of alternating layers of iron and multiwire proportional chambers. The online event selection is performed by a trigger [12], which consists of a hardware stage, based on information from the calorimeter and muon systems, followed by a software stage, which applies a full event reconstruction.

In this analysis, the hardware trigger decision is required to be caused by at least one high- p_T track that is consistent with being a muon. In the software trigger, two well-reconstructed muons with opposite charge are required to form a good-quality vertex and to have an invariant mass consistent with that of the J/ψ meson [4]. The trigger also

requires a significant displacement between the J/ψ vertex and the associated PV of the pp collision.

In the simulation, pp collisions are generated using PYTHIA [13, 14] with a specific LHCb configuration [15]. Decays of hadronic particles are described by EVTGEN [16], in which final-state radiation is generated using PHOTOS [17]. The interaction of the generated particles with the detector, and its response, are implemented using the GEANT4 toolkit [18, 19] as described in ref. [20].

3 Event selection

The same criteria are used to select $B^+ \rightarrow J/\psi \pi^+$ and $B^+ \rightarrow J/\psi K^+$ decays, except for those related to the identification of the final-state hadrons, and consist of a loose preselection followed by a multivariate selection. In the preselection, all three final-state tracks are required to be of good quality and within a fiducial region of the detector acceptance that excludes areas with large asymmetries in the detection efficiencies.

The J/ψ candidates are formed from two oppositely charged particles with p_T greater than 550 MeV/ c , identified as muons and consistent with originating from a common vertex but inconsistent with originating from any PV. The invariant mass of the $\mu^+\mu^-$ pair is required to be within $^{+43}_{-48}$ MeV/ c^2 of the known J/ψ mass [4], then constrained to that value in subsequent stages of the reconstruction. The B^+ candidates are formed by combining each J/ψ candidate with a hadron candidate that has p_T greater than 1 GeV/ c and p greater than 5 GeV/ c and forms a common vertex with the J/ψ . Both the kaon and pion mass hypotheses of the hadron candidates are kept. Each reconstructed B^+ candidate is required to be consistent with originating from a PV. The vector from the corresponding PV to the decay vertex of the B^+ is required to be closely aligned with the momentum vector of the B^+ candidate: the opening angle ϕ between them must satisfy $\cos \phi > 0.999$. To ensure a clean separation between the $B^+ \rightarrow J/\psi \pi^+$ and $B^+ \rightarrow J/\psi K^+$ mass peaks in the $J/\psi \pi^+$ mass spectrum, the decay angle θ_h , defined as the angle between the momentum of the kaon or pion in the B^+ rest frame and the B^+ momentum in the laboratory frame, is required to satisfy $\cos \theta_h < 0$ [8].

The $B^+ \rightarrow J/\psi \pi^+$ and $B^+ \rightarrow J/\psi K^+$ candidates passing the preselection are filtered using the output of a boosted decision tree (BDT) [21, 22] to further suppress combinatorial background. The BDT uses kinematic and topological variables to discriminate between signal and background. These include the impact parameters of the final-state tracks with respect to the PV, as well as those of the J/ψ and the B^+ candidates, the p_T of the final-state hadron and the J/ψ and B^+ candidates, and the decay-length and vertex-fit χ^2 of the B^+ candidate. Given the similarity of their kinematic distributions, the same BDT classifier is used to select both decays. The BDT is trained using a simulated sample of $B^+ \rightarrow J/\psi \pi^+$ decays and a background sample consisting of candidates from the data sample passing the $B^+ \rightarrow J/\psi \pi^+$ preselection with invariant mass in the range 5500–5700 MeV/ c^2 .

Particle identification (PID) criteria are applied to select pion and kaon candidates, with the two hypotheses being mutually exclusive. The requirements on the BDT response

and PID are chosen to maximise the figure of merit for the decay $B^+ \rightarrow J/\psi \pi^+$, defined as $N_\pi/\sqrt{N_{\text{tot}}}$, where N_{tot} is the total number of $B^+ \rightarrow J/\psi \pi^+$ candidates within ± 3 times the mass resolution around the known B^+ mass. Here N_π refers to the $B^+ \rightarrow J/\psi \pi^+$ signal yield and is estimated to be $(N_{\text{tot}} - N_{\text{comb}})/(1 + 1/(r_{\text{eff}} \mathcal{R}_{\pi/K}))$, where the value of $\mathcal{R}_{\pi/K}$ is given in eq. (1.1), N_{comb} is the number of combinatorial background events in the $B^+ \rightarrow J/\psi \pi^+$ signal region extrapolated from the region 5340–5580 MeV/ c^2 passing the PID selection, and r_{eff} is the ratio of the efficiencies for $B^+ \rightarrow J/\psi \pi^+$ and $B^+ \rightarrow J/\psi K^+$ events to pass the $B^+ \rightarrow J/\psi \pi^+$ selection and fall in the signal window, estimated from simulation. After this optimisation, the BDT rejects more than 85% of the combinatorial background and retains around 92% of $B^+ \rightarrow J/\psi h^+$ events, where $h = \pi, K$. The particle identification requirement has an efficiency of about 97% for $B^+ \rightarrow J/\psi \pi^+$ and 69% for $B^+ \rightarrow J/\psi K^+$. The fraction of events in which more than one candidate passes the selection is negligible.

4 Signal yield determination

The signal yields $N_{J/\psi h}$ and raw charge asymmetries $A_{J/\psi h}^{\text{raw}}$ of the two decay modes are determined from independent unbinned extended maximum likelihood fits to the invariant mass distributions of $B^+ \rightarrow J/\psi h^+$ and $B^- \rightarrow J/\psi h^-$. Denoting the signal yield for $B^\pm \rightarrow J/\psi h^\pm$ by $N_{J/\psi h^\pm}$, $N_{J/\psi h}$ is the sum of $B^- \rightarrow J/\psi \pi^-$ and $B^+ \rightarrow J/\psi \pi^+$, and $A_{J/\psi h}^{\text{raw}}$ is defined as

$$A_{J/\psi h}^{\text{raw}} = \frac{N_{J/\psi h^-} - N_{J/\psi h^+}}{N_{J/\psi h^-} + N_{J/\psi h^+}}. \quad (4.1)$$

The fits use $B^+ \rightarrow J/\psi \pi^+$ candidates in the range 5000–5600 MeV/ c^2 and $B^+ \rightarrow J/\psi K^+$ candidates in the range 5000–5700 MeV/ c^2 . The B^+ and B^- samples are fitted simultaneously, as shown in figures 2 and 3. Table 1 summarizes the fit results for the parameters of interest. In each fit, the signal shape is modelled by a Hypatia function [23]. The most probable value and the resolution of the Hypatia function are allowed to vary in the fit, while the tail parameters are fixed to values determined from fits to simulated events. The hadron misidentification background in the $B^+ \rightarrow J/\psi \pi^+$ sample, arising from $B^+ \rightarrow J/\psi K^+$ decays in which the kaon is misidentified as a pion, is described by a double-sided Crystal Ball (DSCB) function whose parameters, except for the most probable value and the core width, are fixed to values determined from fits to simulated events. The misidentification background due to $B^+ \rightarrow J/\psi \pi^+$ decays in which the pion is misidentified as a kaon is neglected in the baseline fit; a systematic uncertainty due to this assumption is assigned, as discussed in section 6. The combinatorial background is modelled by an exponential function whose shape parameter is left free in the fit. The background due to partially reconstructed B -meson decays such as $B \rightarrow J/\psi h \pi$ is described by an ARGUS function [24] convolved with a Gaussian function, with all parameters allowed to vary in the fit. Contributions from the highly suppressed $B^+ \rightarrow K^+ \mu^+ \mu^-$ [4] and $B^+ \rightarrow \pi^+ \mu^+ \mu^-$ [25] decays are negligible.

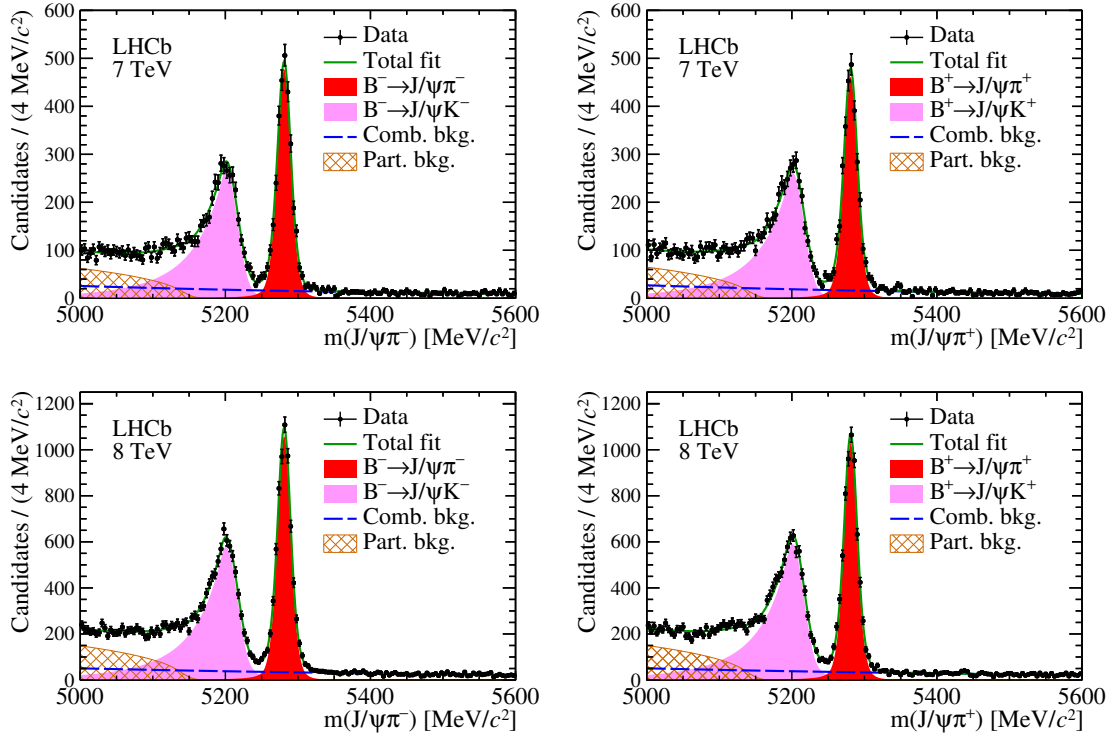


Figure 2. Invariant mass distributions of (left) $B^- \rightarrow J/\psi \pi^-$ and (right) $B^+ \rightarrow J/\psi \pi^+$ candidates with the result of the fit superimposed, for data collected at (top) 7 TeV and (bottom) 8 TeV.

	7 TeV	8 TeV
$N_{J/\psi \pi}$	6011 ± 89	$13\,103 \pm 130$
$N_{J/\psi K}$	$107\,783 \pm 332$	$243\,119 \pm 499$
$A_{J/\psi \pi}^{\text{raw}}$	$(1.64 \pm 1.39) \times 10^{-2}$	$(1.35 \pm 0.94) \times 10^{-2}$
$A_{J/\psi K}^{\text{raw}}$	$(-1.65 \pm 0.31) \times 10^{-2}$	$(-1.27 \pm 0.20) \times 10^{-2}$

Table 1. Signal yields and raw charge asymmetries determined from the fits, which are described in the text. The uncertainties are statistical.

5 Efficiency corrections

The ratio of the $B^+ \rightarrow J/\psi \pi^+$ and $B^+ \rightarrow J/\psi K^+$ branching fractions is measured separately for the 7 and 8 TeV samples, and is calculated as

$$\mathcal{R}_{\pi/K} = \frac{N_{J/\psi \pi}}{N_{J/\psi K}} \times \frac{\varepsilon_{J/\psi K}}{\varepsilon_{J/\psi \pi}}, \quad (5.1)$$

where $\varepsilon_{J/\psi \pi}$ and $\varepsilon_{J/\psi K}$ denote the total efficiencies of selecting the two modes, each taking into account the geometrical acceptance of the detector, the trigger, the reconstruction and preselection, the hadron PID, the BDT selection and the fiducial selection. The hadron PID efficiencies are determined using $D^{*+} \rightarrow D^0(\rightarrow K^- \pi^+) \pi^+$ calibration data [26]. Kaons and pions in the calibration samples are weighted to reproduce the momentum and pseu-

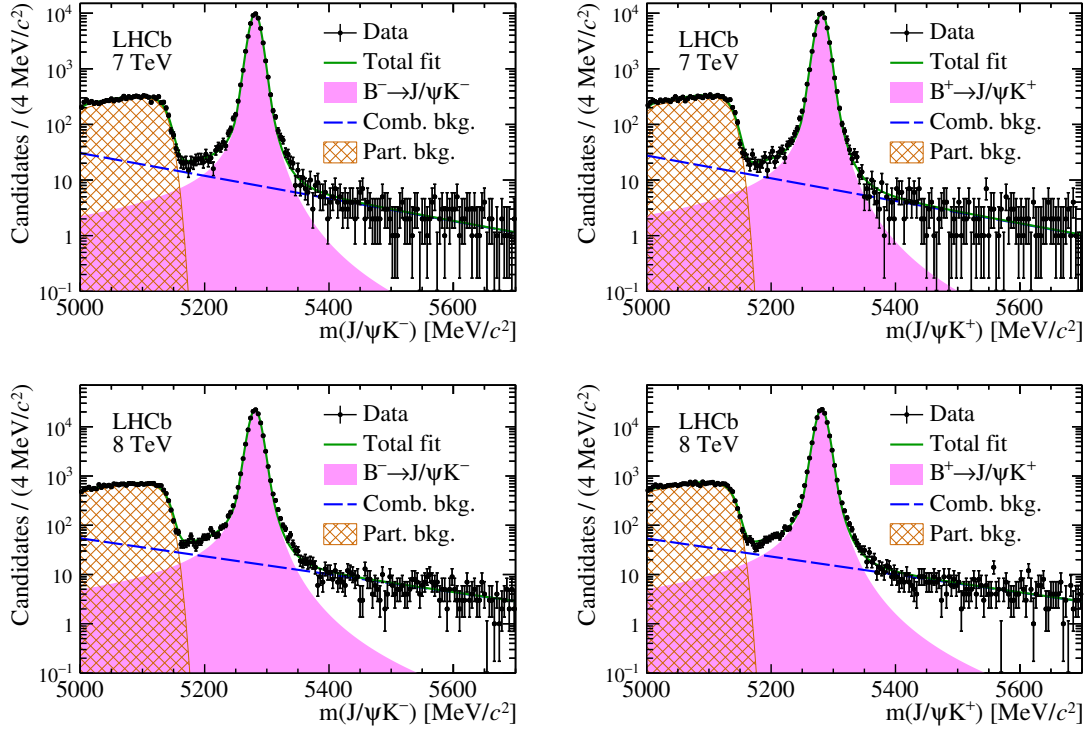


Figure 3. Invariant mass distributions of (left) $B^- \rightarrow J/\psi K^-$ and (right) $B^+ \rightarrow J/\psi K^+$ candidates with the result of the fit superimposed, for data collected at (top) 7 TeV and (bottom) 8 TeV, where the $B^\pm \rightarrow J/\psi \pi^\pm$ contributions are neglected.

dorapidity distributions of those from $B^+ \rightarrow J/\psi K^+$ and $B^+ \rightarrow J/\psi \pi^+$ decays. All other efficiencies are estimated using simulated signal events. The simulated events are weighted such that their kinematic distributions match those of the background-subtracted data, which is obtained using the *sPlot* technique [27]. The efficiency ratio, $\varepsilon_{J/\psi \pi}/\varepsilon_{J/\psi K}$, is estimated to be 1.43 ± 0.01 for the 7 TeV data and 1.42 ± 0.01 for 8 TeV, with the difference from unity being mainly due to the PID selections for the two decays.

The difference in CP asymmetries of $B^+ \rightarrow J/\psi \pi^+$ and $B^+ \rightarrow J/\psi K^+$ is calculated as

$$\begin{aligned}
 \Delta \mathcal{A}^{\text{CP}} &= \Delta A^{\text{raw}} - \Delta A^{\text{eff}}, \\
 \Delta A^{\text{raw}} &\equiv A_{J/\psi \pi}^{\text{raw}} - A_{J/\psi K}^{\text{raw}}, \\
 \Delta A^{\text{eff}} &\equiv A_{J/\psi \pi}^{\text{eff}} - A_{J/\psi K}^{\text{eff}},
 \end{aligned} \tag{5.2}$$

where $A_{J/\psi \pi}^{\text{eff}}$ and $A_{J/\psi K}^{\text{eff}}$ are the efficiency asymmetries between B^- and B^+ decays. The asymmetry difference ΔA^{eff} arises from the particle detection efficiency, hadron PID, BDT selection and fiducial selection. The main sources of asymmetry are the detection efficiency and hadron PID, as described below.

The PID efficiency asymmetries of $B^+ \rightarrow J/\psi \pi^+$ and $B^+ \rightarrow J/\psi K^+$ are estimated separately using the $D^{*+} \rightarrow D^0(\rightarrow K^- \pi^+) \pi^+$ calibration sample mentioned above, and their difference is taken as a contribution to ΔA^{eff} . The average detection asymmetry between π^- and π^+ in $B^+ \rightarrow J/\psi \pi^+$ is denoted A_π^{det} , and that between K^- and K^+ in

$B^+ \rightarrow J/\psi K^+$ is likewise denoted A_K^{det} . Following the method in ref. [28], the difference $A_\pi^{\text{det}} - A_K^{\text{det}}$ can be approximated by the combined detection asymmetry between $\pi^- K^+$ and $\pi^+ K^-$, denoted $A_{\pi\bar{K}}^{\text{det}}$, which is calculated as

$$A_\pi^{\text{det}} - A_K^{\text{det}} \approx A_{\pi\bar{K}}^{\text{det}} = A_{D^- \rightarrow K^+ \pi^- \pi^-}^{\text{raw}} - A_{D^- \rightarrow K_S^0 \pi^-}^{\text{raw}} + A_{K_S^0}^{\text{det}}. \quad (5.3)$$

Here $A_{D^- \rightarrow K^+ \pi^- \pi^-}^{\text{raw}}$ and $A_{D^- \rightarrow K_S^0 \pi^-}^{\text{raw}}$ are the raw charge asymmetries measured in the decays $D^- \rightarrow K^+ \pi^- \pi^-$ and $D^- \rightarrow K_S^0 \pi^-$. The D^\mp production asymmetry cancels in the difference between the two raw asymmetries, and the CP asymmetries in Cabibbo-favoured charm decays are assumed to be negligible. The $D^- \rightarrow K^+ \pi^- \pi^-$ decays are weighted to match the distributions of p_T and rapidity (y) of kaons in the $B^+ \rightarrow J/\psi K^+$ decays. The $D^- \rightarrow K_S^0 \pi^-$ decays are then weighted to match the kinematic distributions of the $D^- \rightarrow K^+ \pi^- \pi^-$ sample such that the p_T and y distributions of the D^- agree between the two channels, as do the p_T distributions of the π^- (with one pion chosen at random in the case of $D^- \rightarrow K^+ \pi^- \pi^-$). The term $A_{K_S^0}^{\text{det}}$ is a small correction for the effects of CP violation in $K^0 - \bar{K}^0$ mixing and the different interaction cross-sections of K^0 and \bar{K}^0 with the detector material [29]. The asymmetry $A_{\pi\bar{K}}^{\text{det}}$ is evaluated to be $(1.10 \pm 0.22) \times 10^{-2}$ and $(0.77 \pm 0.10) \times 10^{-2}$ for the 7 and 8 TeV data, respectively. The overall difference in efficiency asymmetry, ΔA^{eff} , is estimated to be $(1.37 \pm 0.56) \times 10^{-2}$ for the 7 TeV data, and $(0.84 \pm 0.43) \times 10^{-2}$ for 8 TeV .

6 Systematic uncertainties

The data-taking conditions were different for the 7 and 8 TeV data, and therefore the systematic uncertainties, summarised in table 2, are computed separately for the two samples. The relative uncertainties are quoted for the $\mathcal{R}_{\pi/K}$ measurement and absolute uncertainties are quoted for the $\Delta \mathcal{A}^{\text{CP}}$ measurement. The systematic uncertainties can be divided into two groups, either associated with the mass fit or with the efficiency. For each systematic uncertainty associated with the mass fit, a fit with an alternative model is performed and the differences in the mean values of $\mathcal{R}_{\pi/K}$ and $\Delta \mathcal{A}^{\text{CP}}$ are taken as the corresponding systematic uncertainties. The alternative fits are performed with the same sets of parameters floating or fixed as in nominal fit. In each case, the uncertainties are quoted separately for the 7 and 8 TeV data.

The baseline signal model is a Hypatia function. Changing this to a histogram representing the simulated signal mass distribution convolved with a Gaussian function, to correct for mismatch in resolution between data and simulation, leads to relative uncertainties of 0.39% and 0.25% for $\mathcal{R}_{\pi/K}$ for the 7 and 8 TeV data and absolute uncertainties of 0.03×10^{-2} and less than 0.01×10^{-2} for $\Delta \mathcal{A}^{\text{CP}}$.

The baseline model for the misidentification background in the $B^+ \rightarrow J/\psi \pi^+$ sample is a DSCB function with tail parameters obtained from the simulation. Alternative models are constructed by varying the tail parameter values to match those expected for different pion selection requirements, or by using a histogram convolved with a Gaussian function as was done for the signal model. The results from different alternative models are summed in

quadrature. The resulting relative systematic uncertainties on $\mathcal{R}_{\pi/K}$ are 0.44% and 0.38%, and the estimated systematic uncertainties on $\Delta\mathcal{A}^{\text{CP}}$ are 0.01×10^{-2} and 0.02×10^{-2} .

The most probable values and the resolution parameters of the signal and misidentification background models are assumed to be the same for B^+ and B^- decays in the baseline fits. Treating the parameters separately for B^+ and B^- decays leads to differences (taken as estimates of the associated uncertainties) of 0.04×10^{-2} and 0.05×10^{-2} for $\Delta\mathcal{A}^{\text{CP}}$ and 0.04% and 0.02% for $\mathcal{R}_{\pi/K}$.

The baseline model for the combinatorial background is an exponential function. Adding a linear component to this model shifts $\mathcal{R}_{\pi/K}$ by 0.52% and 0.20%, and changes $\Delta\mathcal{A}^{\text{CP}}$ by 0.04×10^{-2} and 0.01×10^{-2} .

The baseline fits are performed in mass ranges above $5000 \text{ MeV}/c^2$, where contamination from the partially reconstructed background is expected up to $5150 \text{ MeV}/c^2$. The alternative fits are performed in narrower ranges starting from $5150 \text{ MeV}/c^2$, where partially reconstructed background can be neglected. The value of $\mathcal{R}_{\pi/K}$ is found to change by 0.20% and 0.33%, and that of $\Delta\mathcal{A}^{\text{CP}}$ by 0.04×10^{-2} and 0.01×10^{-2} . Systematic uncertainties equal to these shifts are assigned.

The PID efficiencies are calibrated using $D^{*+} \rightarrow D^0(\rightarrow K^-\pi^+)\pi^+$ decays selected without applying hadron PID requirements. The efficiency depends on the momentum and pseudorapidity of the track and the track multiplicity in the event, and the calibration is therefore done in bins of those variables. The choice of binning necessarily involves a compromise between the granularity and statistical uncertainty of individual bins. Systematic uncertainties due to the limited number of kinematic bins are evaluated by doubling or halving the number of bins and recalculating the average efficiencies. The resulting deviations from the baseline results are taken as the systematic uncertainties: 0.39% and 0.46% for $\mathcal{R}_{\pi/K}$, and 0.06×10^{-2} and 0.01×10^{-2} for $\Delta\mathcal{A}^{\text{CP}}$.

The ratio of BDT efficiencies of the decays $B^+ \rightarrow J/\psi\pi^+$ and $B^+ \rightarrow J/\psi K^+$ is estimated with simulated samples of signal events, which are weighted to remove differences in the distributions of the BDT input variables between the simulation and data. Relative systematic uncertainties of 0.01% and 0.02% are assigned to $\mathcal{R}_{\pi/K}$, to account for statistical uncertainties on the weights used in the efficiency calculation.

The ratio of trigger efficiencies of the decays $B^+ \rightarrow J/\psi\pi^+$ and $B^+ \rightarrow J/\psi K^+$ is determined from simulation and validated with a control sample of $J/\psi \rightarrow \mu^+\mu^-$ decays [12]. Relative differences of 0.33% and 0.38% are found between the values of this ratio estimated with data and with simulation, which are taken as the corresponding systematic uncertainties on $\mathcal{R}_{\pi/K}$.

Samples of D^+ decays are used to determine the difference between the kaon and pion detection efficiency asymmetries. However, the kinematic distributions of the pions and kaons in the D^+ samples may differ from those of the signal $B^+ \rightarrow J/\psi h^+$ samples, and the efficiency asymmetries may vary with the particle kinematics. To assess the scale of this effect, samples of $D^+ \rightarrow K^-\pi^+\pi^+$ events are weighted such that the distribution of the momentum of the kaon matches that of $B^+ \rightarrow J/\psi K^+$, leading to a pion detection asymmetry of 0.12×10^{-2} for both 7 and 8 TeV data. This is taken as a systematic uncertainty.

Sources	$\mathcal{R}_{\pi/K}$ (7 TeV) [%]	$\mathcal{R}_{\pi/K}$ (8 TeV) [%]	$\Delta\mathcal{A}^{\text{CP}}$ (7 TeV) [$\times 10^{-2}$]	$\Delta\mathcal{A}^{\text{CP}}$ (8 TeV) [$\times 10^{-2}$]
Signal model	0.39	0.25	0.03	—
Mis-ID background	0.44	0.38	0.01	0.02
B^\pm parameters	0.04	0.02	0.04	0.05
Comb. background	0.52	0.20	0.04	0.01
Part. reco. background	0.20	0.33	0.04	0.01
PID efficiency	0.39	0.46	0.06	0.01
BDT efficiency	0.01	0.02	—	—
Trigger efficiency	0.33	0.38	—	—
Detection asymmetry	—	—	0.12	0.12
B^\pm prod. asymmetry	—	—	0.02	0.04
K/π interaction	0.03	0.03	—	—
Total	1.01	0.83	0.15	0.14

Table 2. Relative systematic uncertainties (%) for $\mathcal{R}_{\pi/K}$ and absolute systematic uncertainties ($\times 10^{-2}$) for $\Delta\mathcal{A}^{\text{CP}}$. The uncertainties are quoted separately for the 7 and 8 TeV data. The dashes indicate negligible uncertainties (zero after rounding to two decimal places).

The production asymmetry of B^+ mesons is a function of the B^+ kinematics. This dependence cancels in the observables considered, provided that $B^+ \rightarrow J/\psi \pi^+$ and $B^+ \rightarrow J/\psi K^+$ decays have the same kinematic distributions. Good agreement is found between the p_T distributions of the decays $B^+ \rightarrow J/\psi \pi^+$ and $B^+ \rightarrow J/\psi K^+$, but not for the rapidity distributions. The deviations of the B^+ production asymmetry with and without the weights that match the rapidity distribution in the $B^+ \rightarrow J/\psi \pi^+$ sample to that of the $B^+ \rightarrow J/\psi K^+$ decay, are 0.02×10^{-2} and 0.04×10^{-2} , which are taken as the systematic uncertainties on $\Delta\mathcal{A}^{\text{CP}}$.

A systematic uncertainty of 0.03% on $\mathcal{R}_{\pi/K}$ is assigned to account for imperfect simulation of hadron interactions in the detector, determined from the known interaction cross-sections for pions and kaons and assuming an uncertainty of 10% in the material budget of the detector. Summing all of the above contributions in quadrature, the relative systematic uncertainty on $\mathcal{R}_{\pi/K}$ is 1.01% for the 7 TeV sample and 0.83% for 8 TeV and the absolute uncertainty on $\Delta\mathcal{A}^{\text{CP}}$ is 0.15×10^{-2} for 7 TeV and 0.14×10^{-2} for 8 TeV.

7 Results and conclusion

Using the estimated signal yields, efficiency ratios, raw charge asymmetries and efficiency asymmetries, the ratio of branching fractions and difference in CP asymmetries of the decay modes $B^+ \rightarrow J/\psi \pi^+$ and $B^+ \rightarrow J/\psi K^+$ are measured to be

$$\mathcal{R}_{\pi/K} = \begin{cases} (3.90 \pm 0.06 \pm 0.04) \times 10^{-2} & \text{for 7 TeV} \\ (3.79 \pm 0.04 \pm 0.03) \times 10^{-2} & \text{for 8 TeV}, \end{cases}$$

$$\Delta\mathcal{A}^{\text{CP}} = \begin{cases} (1.92 \pm 1.53 \pm 0.15) \times 10^{-2} & \text{for 7 TeV} \\ (1.77 \pm 1.05 \pm 0.14) \times 10^{-2} & \text{for 8 TeV}. \end{cases}$$

Here the first uncertainties are statistical, which are uncorrelated between the 7 and 8 TeV results, and the second uncertainties are systematic, which are taken to be fully correlated between the 7 and 8 TeV results. The average of the 7 and 8 TeV results, weighting each according to its statistical uncertainty, are

$$\begin{aligned}\mathcal{R}_{\pi/K} &= (3.83 \pm 0.03 \pm 0.03) \times 10^{-2}, \\ \Delta\mathcal{A}^{\text{CP}} &= (1.82 \pm 0.86 \pm 0.14) \times 10^{-2}.\end{aligned}$$

The LHCb collaboration has recently reported the CP asymmetry $\mathcal{A}^{\text{CP}}(B^+ \rightarrow J/\psi K^+) = (0.09 \pm 0.27 \pm 0.07) \times 10^{-2}$ [9], where the first uncertainty is statistical and the second systematic. The sample analysed in ref. [9] is statistically correlated with that used in this analysis, but the correlation is only partial due to the use of different trigger requirements. The correlation coefficient between the statistical uncertainties of the two analyses is found to be -4.8% . The systematic uncertainty on $\mathcal{A}^{\text{CP}}(B^+ \rightarrow J/\psi K^+)$ is taken to be uncorrelated with that on the $\Delta\mathcal{A}^{\text{CP}}$ measurement. Therefore the CP asymmetry in the decay $B^+ \rightarrow J/\psi \pi^+$ is

$$\mathcal{A}^{\text{CP}}(B^+ \rightarrow J/\psi \pi^+) = \Delta\mathcal{A}^{\text{CP}} + \mathcal{A}^{\text{CP}}(B^+ \rightarrow J/\psi K^+) = (1.91 \pm 0.89 \pm 0.16) \times 10^{-2}.$$

This is the most precise determination of $\mathcal{A}^{\text{CP}}(B^+ \rightarrow J/\psi \pi^+)$ to date, and it supersedes the previous LHCb result [8]. The $\mathcal{R}_{\pi/K}$ and $\mathcal{A}^{\text{CP}}(B^+ \rightarrow J/\psi \pi^+)$ measurements can be combined with measurements of decay rates and CP asymmetries in other $b \rightarrow c\bar{c}d$ decays, such as $B^0 \rightarrow J/\psi \pi^0$, to understand the effect of loop contributions in $b \rightarrow c\bar{c}s$ decays using $SU(3)$ flavour symmetry [2, 3].

Acknowledgments

We express our gratitude to our colleagues in the CERN accelerator departments for the excellent performance of the LHC. We thank the technical and administrative staff at the LHCb institutes. We acknowledge support from CERN and from the national agencies: CAPES, CNPq, FAPERJ and FINEP (Brazil); NSFC (China); CNRS/IN2P3 (France); BMBF, DFG and MPG (Germany); INFN (Italy); FOM and NWO (The Netherlands); MNiSW and NCN (Poland); MEN/IFA (Romania); MinES and FASO (Russia); MinECo (Spain); SNSF and SER (Switzerland); NASU (Ukraine); STFC (United Kingdom); NSF (U.S.A.). We acknowledge the computing resources that are provided by CERN, IN2P3 (France), KIT and DESY (Germany), INFN (Italy), SURF (The Netherlands), PIC (Spain), GridPP (United Kingdom), RRCKI and Yandex LLC (Russia), CSCS (Switzerland), IFIN-HH (Romania), CBPF (Brazil), PL-GRID (Poland) and OSC (U.S.A.). We are indebted to the communities behind the multiple open source software packages on which we depend. Individual groups or members have received support from AvH Foundation (Germany), EPLANET, Marie Skłodowska-Curie Actions and ERC (European Union), Conseil Général de Haute-Savoie, Labex ENIGMASS and OCEVU, Région Auvergne (France), RFBR and Yandex LLC (Russia), GVA, XuntaGal and GENCAT (Spain), Herchel Smith Fund, The Royal Society, Royal Commission for the Exhibition of 1851 and the Leverhulme Trust (United Kingdom).

Open Access. This article is distributed under the terms of the Creative Commons Attribution License ([CC-BY 4.0](https://creativecommons.org/licenses/by/4.0/)), which permits any use, distribution and reproduction in any medium, provided the original author(s) and source are credited.

References

- [1] I. Dunietz and J.M. Soares, *Direct CP-violation in $b \rightarrow dJ/\psi$ decays*, *Phys. Rev. D* **49** (1994) 5904 [[hep-ph/9312233](#)] [[INSPIRE](#)].
- [2] Z. Ligeti and D.J. Robinson, *Towards more precise determinations of the quark mixing phase β* , *Phys. Rev. Lett.* **115** (2015) 251801 [[arXiv:1507.06671](#)] [[INSPIRE](#)].
- [3] K. De Bruyn and R. Fleischer, *A roadmap to control penguin effects in $B_d^0 \rightarrow J/\psi K_S^0$ and $B_s^0 \rightarrow J/\psi \phi$* , *JHEP* **03** (2015) 145 [[arXiv:1412.6834](#)] [[INSPIRE](#)].
- [4] PARTICLE DATA GROUP collaboration, C. Patrignani et al., *Review of particle physics*, *Chin. Phys. C* **40** (2016) 100001 [[INSPIRE](#)].
- [5] BELLE collaboration, K. Abe et al., *Measurement of branching fractions and charge asymmetries for two-body B meson decays with charmonium*, *Phys. Rev. D* **67** (2003) 032003 [[hep-ex/0211047](#)] [[INSPIRE](#)].
- [6] BABAR collaboration, B. Aubert et al., *Study of $B^\pm \rightarrow J/\psi \pi^\pm$ and $B^\pm \rightarrow J/\psi K^\pm$ decays: measurement of the ratio of branching fractions and search for direct CP-violation*, *Phys. Rev. Lett.* **92** (2004) 241802 [[hep-ex/0401035](#)] [[INSPIRE](#)].
- [7] D0 collaboration, V.M. Abazov et al., *Measurement of direct CP-violation parameters in $B^\pm \rightarrow J/\psi K^\pm$ and $B^\pm \rightarrow J/\psi \pi^\pm$ decays with 10.4 fb^{-1} of Tevatron data*, *Phys. Rev. Lett.* **110** (2013) 241801 [[arXiv:1304.1655](#)] [[INSPIRE](#)].
- [8] LHCb collaboration, *Measurements of the branching fractions and CP asymmetries of $B^\pm \rightarrow J/\psi \pi^\pm$ and $B^\pm \rightarrow \psi(2S) \pi^\pm$ decays*, *Phys. Rev. D* **85** (2012) 091105 [[arXiv:1203.3592](#)] [[INSPIRE](#)].
- [9] LHCb collaboration, *Measurement of the B^\pm production asymmetry and the CP asymmetry in $B^\pm \rightarrow J/\psi K^\pm$ decays*, [arXiv:1701.05501](#) [[LHCb-PAPER-2016-054](#)].
- [10] LHCb collaboration, *The LHCb detector at the LHC*, 2008 *JINST* **3** S08005 [[INSPIRE](#)].
- [11] LHCb collaboration, *LHCb detector performance*, *Int. J. Mod. Phys. A* **30** (2015) 1530022 [[arXiv:1412.6352](#)] [[INSPIRE](#)].
- [12] R. Aaij et al., *The LHCb trigger and its performance in 2011, 2013* *JINST* **8** P04022 [[arXiv:1211.3055](#)] [[INSPIRE](#)].
- [13] T. Sjöstrand, S. Mrenna and P.Z. Skands, *PYTHIA 6.4 physics and manual*, *JHEP* **05** (2006) 026 [[hep-ph/0603175](#)] [[INSPIRE](#)].
- [14] T. Sjöstrand, S. Mrenna and P.Z. Skands, *A brief introduction to PYTHIA 8.1*, *Comput. Phys. Commun.* **178** (2008) 852 [[arXiv:0710.3820](#)] [[INSPIRE](#)].
- [15] LHCb collaboration, *Handling of the generation of primary events in Gauss, the LHCb simulation framework*, *J. Phys. Conf. Ser.* **331** (2011) 032047 [[INSPIRE](#)].
- [16] D.J. Lange, *The EvtGen particle decay simulation package*, *Nucl. Instrum. Meth. A* **462** (2001) 152 [[INSPIRE](#)].

- [17] P. Golonka and Z. Was, *PHOTOS Monte Carlo: a precision tool for QED corrections in Z and W decays*, *Eur. Phys. J. C* **45** (2006) 97 [[hep-ph/0506026](#)] [[INSPIRE](#)].
- [18] GEANT4 collaboration, J. Allison et al., *GEANT4 developments and applications*, *IEEE Trans. Nucl. Sci.* **53** (2006) 270.
- [19] GEANT4 collaboration, S. Agostinelli et al., *GEANT4: a simulation toolkit*, *Nucl. Instrum. Meth. A* **506** (2003) 250 [[INSPIRE](#)].
- [20] LHCb collaboration, *The LHCb simulation application, Gauss: Design, evolution and experience*, *J. Phys. Conf. Ser.* **331** (2011) 032023 [[INSPIRE](#)].
- [21] L. Breiman, J.H. Friedman, R.A. Olshen and C.J. Stone, *Classification and regression trees*, Wadsworth international group, California, Belmont U.S.A. (1984).
- [22] Y. Freund and R. E. Schapire, *A decision-theoretic generalization of on-line learning and an application to boosting*, *J. Comput. Syst. Sci.* **55** (1997) 119.
- [23] D. Martínez Santos and F. Dupertuis, *Mass distributions marginalized over per-event errors*, *Nucl. Instrum. Meth. A* **764** (2014) 150 [[arXiv:1312.5000](#)] [[INSPIRE](#)].
- [24] ARGUS collaboration, H. Albrecht et al., *Search for hadronic $b \rightarrow u$ decays*, *Phys. Lett. B* **241** (1990) 278 [[INSPIRE](#)].
- [25] LHCb collaboration, *First observation of the decay $B^+ \rightarrow \pi^+ \mu^+ \mu^-$* , *JHEP* **12** (2012) 125 [[arXiv:1210.2645](#)] [[INSPIRE](#)].
- [26] L. Anderlini et al., *The PIDCalib package*, CERN-LHCb-PUB-2016-021 (2016).
- [27] M. Pivk and F.R. Le Diberder, *SPlot: a statistical tool to unfold data distributions*, *Nucl. Instrum. Meth. A* **555** (2005) 356 [[physics/0402083](#)] [[INSPIRE](#)].
- [28] LHCb collaboration, *Measurement of indirect CP asymmetries in $D^0 \rightarrow K^- K^+$ and $D^0 \rightarrow \pi^- \pi^+$ decays using semileptonic B decays*, *JHEP* **04** (2015) 043 [[arXiv:1501.06777](#)] [[INSPIRE](#)].
- [29] LHCb collaboration, *Measurement of CP asymmetry in $D^0 \rightarrow K^- K^+$ and $D^0 \rightarrow \pi^- \pi^+$ decays*, *JHEP* **07** (2014) 041 [[arXiv:1405.2797](#)] [[INSPIRE](#)].

The LHCb collaboration

R. Aaij⁴⁰, B. Adeva³⁹, M. Adinolfi⁴⁸, Z. Ajaltouni⁵, S. Akar⁵⁹, J. Albrecht¹⁰, F. Alessio⁴⁰, M. Alexander⁵³, S. Ali⁴³, G. Alkhazov³¹, P. Alvarez Cartelle⁵⁵, A.A. Alves Jr⁵⁹, S. Amato², S. Amerio²³, Y. Amhis⁷, L. An³, L. Anderlini¹⁸, G. Andreassi⁴¹, M. Andreotti^{17,g}, J.E. Andrews⁶⁰, R.B. Appleby⁵⁶, F. Archilli⁴³, P. d'Argent¹², J. Arnau Romeu⁶, A. Artamonov³⁷, M. Artuso⁶¹, E. Aslanides⁶, G. Auriemma²⁶, M. Baalouch⁵, I. Babuschkin⁵⁶, S. Bachmann¹², J.J. Back⁵⁰, A. Badalov³⁸, C. Baesso⁶², S. Baker⁵⁵, V. Balagura^{7,c}, W. Baldini¹⁷, R.J. Barlow⁵⁶, C. Barschel⁴⁰, S. Barsuk⁷, W. Barter⁴⁰, M. Baszczyk²⁷, V. Batozskaya²⁹, B. Batsukh⁶¹, V. Battista⁴¹, A. Bay⁴¹, L. Beaucourt⁴, J. Beddow⁵³, F. Bedeschi²⁴, I. Bediaga¹, L.J. Bel⁴³, V. Belle⁴¹, N. Belloli^{21,i}, K. Belous³⁷, I. Belyaev³², E. Ben-Haim⁸, G. Bencivenni¹⁹, S. Benson⁴³, A. Berezhnoy³³, R. Bernet⁴², A. Bertolin²³, C. Betancourt⁴², F. Betti¹⁵, M.-O. Bettler⁴⁰, M. van Beuzekom⁴³, Ia. Bezshyiko⁴², S. Bifani⁴⁷, P. Billoir⁸, T. Bird⁵⁶, A. Birnkraut¹⁰, A. Bitadze⁵⁶, A. Bizzeti^{18,u}, T. Blake⁵⁰, F. Blanc⁴¹, J. Blouw^{11,†}, S. Blusk⁶¹, V. Bocci²⁶, T. Boettcher⁵⁸, A. Bondar^{36,w}, N. Bondar^{31,40}, W. Bonivento¹⁶, I. Bordyuzhin³², A. Borgheresi^{21,i}, S. Borghi⁵⁶, M. Borisov³⁵, M. Borsato³⁹, F. Bossu⁷, M. Boubdir⁹, T.J.V. Bowcock⁵⁴, E. Bowen⁴², C. Bozzi^{17,40}, S. Braun¹², M. Britsch¹², T. Britton⁶¹, J. Brodzicka⁵⁶, E. Buchanan⁴⁸, C. Burr⁵⁶, A. Bursche², J. Buytaert⁴⁰, S. Cadeddu¹⁶, R. Calabrese^{17,g}, M. Calvi^{21,i}, M. Calvo Gomez^{38,m}, A. Camboni³⁸, P. Campana¹⁹, D.H. Campora Perez⁴⁰, L. Capriotti⁵⁶, A. Carbone^{15,e}, G. Carboni^{25,j}, R. Cardinale^{20,h}, A. Cardini¹⁶, P. Carniti^{21,i}, L. Carson⁵², K. Carvalho Akiba², G. Casse⁵⁴, L. Cassina^{21,i}, L. Castillo Garcia⁴¹, M. Cattaneo⁴⁰, G. Cavallero²⁰, R. Cenci^{24,t}, D. Chamont⁷, M. Charles⁸, Ph. Charpentier⁴⁰, G. Chatzikonstantinidis⁴⁷, M. Chefdeville⁴, S. Chen⁵⁶, S.-F. Cheung⁵⁷, V. Chobanova³⁹, M. Chrzasczcz^{42,27}, X. Cid Vidal³⁹, G. Ciezarek⁴³, P.E.L. Clarke⁵², M. Clemencic⁴⁰, H.V. Cliff⁴⁹, J. Closier⁴⁰, V. Coco⁵⁹, J. Cogan⁶, E. Cogneras⁵, V. Cogoni^{16,40,f}, L. Cojocariu³⁰, G. Collazuol^{23,o}, P. Collins⁴⁰, A. Comerma-Montells¹², A. Contu⁴⁰, A. Cook⁴⁸, G. Coombs⁴⁰, S. Coquereau³⁸, G. Corti⁴⁰, M. Corvo^{17,g}, C.M. Costa Sobral⁵⁰, B. Couturier⁴⁰, G.A. Cowan⁵², D.C. Craik⁵², A. Crocombe⁵⁰, M. Cruz Torres⁶², S. Cunliffe⁵⁵, R. Currie⁵⁵, C. D'Ambrosio⁴⁰, F. Da Cunha Marinho², E. Dall'Occo⁴³, J. Dalseno⁴⁸, P.N.Y. David⁴³, A. Davis³, K. De Bruyn⁶, S. De Capua⁵⁶, M. De Cian¹², J.M. De Miranda¹, L. De Paula², M. De Serio^{14,d}, P. De Simone¹⁹, C.-T. Dean⁵³, D. Decamp⁴, M. Deckenhoff¹⁰, L. Del Buono⁸, M. Demmer¹⁰, A. Dendek²⁸, D. Derkach³⁵, O. Deschamps⁵, F. Dettori⁴⁰, B. Dey²², A. Di Canto⁴⁰, H. Dijkstra⁴⁰, F. Dordei⁴⁰, M. Dorigo⁴¹, A. Dosil Suárez³⁹, A. Dovbnya⁴⁵, K. Dreimanis⁵⁴, L. Dufour⁴³, G. Dujany⁵⁶, K. Dungs⁴⁰, P. Durante⁴⁰, R. Dzhelyadin³⁷, A. Dziurda⁴⁰, A. Dzyuba³¹, N. Déleage⁴, S. Easo⁵¹, M. Ebert⁵², U. Egede⁵⁵, V. Egorychev³², S. Eidelman^{36,w}, S. Eisenhardt⁵², U. Eitschberger¹⁰, R. Ekelhof¹⁰, L. Eklund⁵³, S. Ely⁶¹, S. Esen¹², H.M. Evans⁴⁹, T. Evans⁵⁷, A. Falabella¹⁵, N. Farley⁴⁷, S. Farry⁵⁴, R. Fay⁵⁴, D. Fazzini^{21,i}, D. Ferguson⁵², A. Fernandez Prieto³⁹, F. Ferrari^{15,40}, F. Ferreira Rodrigues², M. Ferro-Luzzi⁴⁰, S. Filippov³⁴, R.A. Fini¹⁴, M. Fiore^{17,g}, M. Fiorini^{17,g}, M. Firlej²⁸, C. Fitzpatrick⁴¹, T. Fiutowski²⁸, F. Fleuret^{7,b}, K. Fohl⁴⁰, M. Fontana^{16,40}, F. Fontanelli^{20,h}, D.C. Forshaw⁶¹, R. Forty⁴⁰, V. Franco Lima⁵⁴, M. Frank⁴⁰, C. Frei⁴⁰, J. Fu^{22,q}, W. Funk⁴⁰, E. Furfaro^{25,j}, C. Färber⁴⁰, A. Gallas Torreira³⁹, D. Galli^{15,e}, S. Gallorini²³, S. Gambetta⁵², M. Gandelman², P. Gandini⁵⁷, Y. Gao³, L.M. Garcia Martin⁶⁹, J. García Pardiñas³⁹, J. Garra Tico⁴⁹, L. Garrido³⁸, P.J. Garsed⁴⁹, D. Gascon³⁸, C. Gaspar⁴⁰, L. Gavardi¹⁰, G. Gazzoni⁵, D. Gerick¹², E. Gersabeck¹², M. Gersabeck⁵⁶, T. Gershon⁵⁰, Ph. Ghez⁴, S. Gianì⁴¹, V. Gibson⁴⁹, O.G. Girard⁴¹, L. Giubega³⁰, K. Gizdov⁵², V.V. Gligorov⁸, D. Golubkov³², A. Golutvin^{55,40}, A. Gomes^{1,a}, I.V. Gorelov³³, C. Gotti^{21,i}, R. Graciani Diaz³⁸, L.A. Granado Cardoso⁴⁰, E. Graugés³⁸, E. Graverini⁴², G. Graziani¹⁸, A. Grecu³⁰, P. Griffith⁴⁷,

L. Grillo^{21,40,i}, B.R. Gruber Cazon⁵⁷, O. Grünberg⁶⁷, E. Gushchin³⁴, Yu. Guz³⁷, T. Gys⁴⁰, C. Göbel⁶², T. Hadavizadeh⁵⁷, C. Hadjivasiliou⁵, G. Haefeli⁴¹, C. Haen⁴⁰, S.C. Haines⁴⁹, S. Hall⁵⁵, B. Hamilton⁶⁰, X. Han¹², S. Hansmann-Menzemer¹², N. Harnew⁵⁷, S.T. Harnew⁴⁸, J. Harrison⁵⁶, M. Hatch⁴⁰, J. He⁶³, T. Head⁴¹, A. Heister⁹, K. Hennessy⁵⁴, P. Henrard⁵, L. Henry⁸, E. van Herwijnen⁴⁰, M. Heß⁶⁷, A. Hicheur², D. Hill⁵⁷, C. Hombach⁵⁶, H. Hopchev⁴¹, W. Hulsbergen⁴³, T. Humair⁵⁵, M. Hushchyn³⁵, D. Hutchcroft⁵⁴, M. Idzik²⁸, P. Ilten⁵⁸, R. Jacobsson⁴⁰, A. Jaeger¹², J. Jalocha⁵⁷, E. Jans⁴³, A. Jawahery⁶⁰, F. Jiang³, M. John⁵⁷, D. Johnson⁴⁰, C.R. Jones⁴⁹, C. Joram⁴⁰, B. Jost⁴⁰, N. Jurik⁵⁷, S. Kandybei⁴⁵, M. Karacson⁴⁰, J.M. Kariuki⁴⁸, S. Karodia⁵³, M. Kecke¹², M. Kelsey⁶¹, M. Kenzie⁴⁹, T. Ketel⁴⁴, E. Khairullin³⁵, B. Khanji¹², C. Khurewathanakul⁴¹, T. Kirn⁹, S. Klaver⁵⁶, K. Klimaszewski²⁹, S. Kolliiev⁴⁶, M. Kolpin¹², I. Komarov⁴¹, R.F. Koopman⁴⁴, P. Koppenburg⁴³, A. Kosmyntseva³², A. Kozachuk³³, M. Kozeiha⁵, L. Kravchuk³⁴, K. Kreplin¹², M. Kreps⁵⁰, P. Krokovny^{36,w}, F. Kruse¹⁰, W. Krzemien²⁹, W. Kucewicz^{27,l}, M. Kucharczyk²⁷, V. Kudryavtsev^{36,w}, A.K. Kuonen⁴¹, K. Kurek²⁹, T. Kvaratskheliya^{32,40}, D. Lacarrere⁴⁰, G. Lafferty⁵⁶, A. Lai¹⁶, G. Lanfranchi¹⁹, C. Langenbruch⁹, T. Latham⁵⁰, C. Lazzeroni⁴⁷, R. Le Gac⁶, J. van Leerdam⁴³, A. Leflat^{33,40}, J. Lefrançois⁷, R. Lefèvre⁵, F. Lemaitre⁴⁰, E. Lemos Cid³⁹, O. Leroy⁶, T. Lesiak²⁷, B. Leverington¹², T. Li³, Y. Li⁷, T. Likhomanenko^{35,68}, R. Lindner⁴⁰, C. Linn⁴⁰, F. Lionetto⁴², X. Liu³, D. Loh⁵⁰, I. Longstaff⁵³, J.H. Lopes², D. Lucchesi^{23,o}, M. Lucio Martinez³⁹, H. Luo⁵², A. Lupato²³, E. Luppi^{17,g}, O. Lupton⁴⁰, A. Lusiani²⁴, X. Lyu⁶³, F. Machefert⁷, F. Maciuc³⁰, O. Maev³¹, K. Maguire⁵⁶, S. Malde⁵⁷, A. Malinin⁶⁸, T. Maltsev³⁶, G. Manca^{16,f}, G. Mancinelli⁶, P. Manning⁶¹, J. Maratas^{5,v}, J.F. Marchand⁴, U. Marconi¹⁵, C. Marin Benito³⁸, M. Marinangeli⁴¹, P. Marino^{24,t}, J. Marks¹², G. Martellotti²⁶, M. Martin⁶, M. Martinelli⁴¹, D. Martinez Santos³⁹, F. Martinez Vidal⁶⁹, D. Martins Tostes², L.M. Massacrier⁷, A. Massafferri¹, R. Matev⁴⁰, A. Mathad⁵⁰, Z. Mathe⁴⁰, C. Matteuzzi²¹, A. Mauri⁴², E. Maurice^{7,b}, B. Maurin⁴¹, A. Mazurov⁴⁷, M. McCann^{55,40}, A. McNab⁵⁶, R. McNulty¹³, B. Meadows⁵⁹, F. Meier¹⁰, M. Meissner¹², D. Melnychuk²⁹, M. Merk⁴³, A. Merli^{22,q}, E. Michielin²³, D.A. Milanes⁶⁶, M.-N. Minard⁴, D.S. Mitzel¹², A. Mogini⁸, J. Molina Rodriguez¹, I.A. Monroy⁶⁶, S. Monteil⁵, M. Morandin²³, P. Morawski²⁸, A. Mordà⁶, M.J. Morello^{24,t}, O. Morgunova⁶⁸, J. Moron²⁸, A.B. Morris⁵², R. Mountain⁶¹, F. Muheim⁵², M. Mulder⁴³, M. Mussini¹⁵, D. Müller⁵⁶, J. Müller¹⁰, K. Müller⁴², V. Müller¹⁰, P. Naik⁴⁸, T. Nakada⁴¹, R. Nandakumar⁵¹, A. Nandi⁵⁷, I. Nasteva², M. Needham⁵², N. Neri²², S. Neubert¹², N. Neufeld⁴⁰, M. Neuner¹², T.D. Nguyen⁴¹, C. Nguyen-Mau^{41,n}, S. Nieswand⁹, R. Niet¹⁰, N. Nikitin³³, T. Nikodem¹², A. Nogay⁶⁸, A. Novoselov³⁷, D.P. O'Hanlon⁵⁰, A. Oblakowska-Mucha²⁸, V. Obraztsov³⁷, S. Ogilvy¹⁹, R. Oldeman^{16,f}, C.J.G. Onderwater⁷⁰, J.M. Otalora Goicochea², A. Otto⁴⁰, P. Owen⁴², A. Oyanguren⁶⁹, P.R. Pais⁴¹, A. Palano^{14,d}, F. Palombo^{22,q}, M. Palutan¹⁹, A. Papanestis⁵¹, M. Pappagallo^{14,d}, L.L. Pappalardo^{17,g}, W. Parker⁶⁰, C. Parkes⁵⁶, G. Passaleva¹⁸, A. Pastore^{14,d}, G.D. Patel⁵⁴, M. Patel⁵⁵, C. Patrignani^{15,e}, A. Pearce⁴⁰, A. Pellegrino⁴³, G. Penso²⁶, M. Pepe Altarelli⁴⁰, S. Perazzini⁴⁰, P. Perret⁵, L. Pescatore⁴⁷, K. Petridis⁴⁸, A. Petrolini^{20,h}, A. Petrov⁶⁸, M. Petruzzo^{22,q}, E. Picatoste Olloqui³⁸, B. Pietrzyk⁴, M. Pikies²⁷, D. Pinci²⁶, A. Pistone²⁰, A. Piucci¹², V. Placinta³⁰, S. Playfer⁵², M. Plo Casasus³⁹, T. Poikela⁴⁰, F. Polci⁸, A. Poluektov^{50,36}, I. Polyakov⁶¹, E. Polcarpo², G.J. Pomery⁴⁸, A. Popov³⁷, D. Popov^{11,40}, B. Popovici³⁰, S. Poslavskii³⁷, C. Potterat², E. Price⁴⁸, J.D. Price⁵⁴, J. Prisciandaro^{39,40}, A. Pritchard⁵⁴, C. Prouve⁴⁸, V. Pugatch⁴⁶, A. Puig Navarro⁴², G. Punzi^{24,p}, W. Qian⁵⁰, R. Quagliani^{7,48}, B. Rachwal²⁷, J.H. Rademacker⁴⁸, M. Rama²⁴, M. Ramos Pernas³⁹, M.S. Rangel², I. Raniuk⁴⁵, F. Ratnikov³⁵, G. Raven⁴⁴, F. Redi⁵⁵, S. Reichert¹⁰, A.C. dos Reis¹, C. Remon Alepuz⁶⁹, V. Renaudin⁷, S. Ricciardi⁵¹, S. Richards⁴⁸, M. Rihl⁴⁰, K. Rinnert⁵⁴, V. Rives Molina³⁸, P. Robbe^{7,40}, A.B. Rodrigues¹, E. Rodrigues⁵⁹, J.A. Rodriguez Lopez⁶⁶, P. Rodriguez Perez^{56,†}, A. Rogozhnikov³⁵, S. Roiser⁴⁰, A. Rollings⁵⁷, V. Romanovskiy³⁷,

A. Romero Vidal³⁹, J.W. Ronayne¹³, M. Rotondo¹⁹, M.S. Rudolph⁶¹, T. Ruf⁴⁰, P. Ruiz Valls⁶⁹, J.J. Saborido Silva³⁹, E. Sadykhov³², N. Sagidova³¹, B. Saitta^{16,f}, V. Salustino Guimaraes¹, C. Sanchez Mayordomo⁶⁹, B. Sanmartin Sedes³⁹, R. Santacesaria²⁶, C. Santamarina Rios³⁹, M. Santimaria¹⁹, E. Santovetti^{25,j}, A. Sarti^{19,k}, C. Satriano^{26,s}, A. Satta²⁵, D.M. Saunders⁴⁸, D. Savrina^{32,33}, S. Schael⁹, M. Schellenberg¹⁰, M. Schiller⁵³, H. Schindler⁴⁰, M. Schlupp¹⁰, M. Schmelling¹¹, T. Schmelzer¹⁰, B. Schmidt⁴⁰, O. Schneider⁴¹, A. Schopper⁴⁰, K. Schubert¹⁰, M. Schubiger⁴¹, M.-H. Schune⁷, R. Schwemmer⁴⁰, B. Sciascia¹⁹, A. Sciubba^{26,k}, A. Semennikov³², A. Sergi⁴⁷, N. Serra⁴², J. Serrano⁶, L. Sestini²³, P. Seyfert²¹, M. Shapkin³⁷, I. Shapoval⁴⁵, Y. Shcheglov³¹, T. Shears⁵⁴, L. Shekhtman^{36,w}, V. Shevchenko⁶⁸, B.G. Siddi^{17,40}, R. Silva Coutinho⁴², L. Silva de Oliveira², G. Simi^{23,o}, S. Simone^{14,d}, M. Sirendi⁴⁹, N. Skidmore⁴⁸, T. Skwarnicki⁶¹, E. Smith⁵⁵, I.T. Smith⁵², J. Smith⁴⁹, M. Smith⁵⁵, H. Snoek⁴³, I. Soares Lavra¹, M.D. Sokoloff⁵⁹, F.J.P. Soler⁵³, B. Souza De Paula², B. Spaan¹⁰, P. Spradlin⁵³, S. Sridharan⁴⁰, F. Stagni⁴⁰, M. Stahl¹², S. Stahl⁴⁰, P. Stefkova⁴¹, S. Stefkova⁵⁵, O. Steinkamp⁴², S. Stemmler¹², O. Stenyakin³⁷, H. Stevens¹⁰, S. Stevenson⁵⁷, S. Stoica³⁰, S. Stone⁶¹, B. Storaci⁴², S. Stracka^{24,p}, M. Straticiu³⁰, U. Straumann⁴², L. Sun⁶⁴, W. Sutcliffe⁵⁵, K. Swientek²⁸, V. Syropoulos⁴⁴, M. Szczekowski²⁹, T. Szumlak²⁸, S. T'Jampens⁴, A. Tayduganov⁶, T. Tekampe¹⁰, G. Tellarini^{17,g}, F. Teubert⁴⁰, E. Thomas⁴⁰, J. van Tilburg⁴³, M.J. Tilley⁵⁵, V. Tisserand⁴, M. Tobin⁴¹, S. Tolk⁴⁹, L. Tomassetti^{17,g}, D. Tonelli⁴⁰, S. Topp-Joergensen⁵⁷, F. Toriello⁶¹, E. Tournefier⁴, S. Tourneur⁴¹, K. Trabelsi⁴¹, M. Traill⁵³, M.T. Tran⁴¹, M. Tresch⁴², A. Trisovic⁴⁰, A. Tsaregorodtsev⁶, P. Tsopelas⁴³, A. Tully⁴⁹, N. Tuning⁴³, A. Ukleja²⁹, A. Ustyuzhanin³⁵, U. Uwer¹², C. Vacca^{16,f}, V. Vagnoni^{15,40}, A. Valassi⁴⁰, S. Valat⁴⁰, G. Valenti¹⁵, R. Vazquez Gomez¹⁹, P. Vazquez Regueiro³⁹, S. Vecchi¹⁷, M. van Veghel⁴³, J.J. Velthuis⁴⁸, M. Veltri^{18,r}, G. Veneziano⁵⁷, A. Venkateswaran⁶¹, M. Vernet⁵, M. Vesterinen¹², J.V. Viana Barbosa⁴⁰, B. Viaud⁷, D. Vieira⁶³, M. Vieites Diaz³⁹, H. Viemann⁶⁷, X. Vilasis-Cardona^{38,m}, M. Vitti⁴⁹, V. Volkov³³, A. Vollhardt⁴², B. Voneki⁴⁰, A. Vorobyev³¹, V. Vorobyev^{36,w}, C. Voß⁹, J.A. de Vries⁴³, C. Vázquez Sierra³⁹, R. Waldi⁶⁷, C. Wallace⁵⁰, R. Wallace¹³, J. Walsh²⁴, J. Wang⁶¹, D.R. Ward⁴⁹, H.M. Wark⁵⁴, N.K. Watson⁴⁷, D. Websdale⁵⁵, A. Weiden⁴², M. Whitehead⁴⁰, J. Wicht⁵⁰, G. Wilkinson^{57,40}, M. Wilkinson⁶¹, M. Williams⁴⁰, M.P. Williams⁴⁷, M. Williams⁵⁸, T. Williams⁴⁷, F.F. Wilson⁵¹, J. Wimberley⁶⁰, J. Wishahi¹⁰, W. Wislicki²⁹, M. Witek²⁷, G. Wormser⁷, S.A. Wotton⁴⁹, K. Wraight⁵³, K. Wyllie⁴⁰, Y. Xie⁶⁵, Z. Xing⁶¹, Z. Xu⁴¹, Z. Yang³, Y. Yao⁶¹, H. Yin⁶⁵, J. Yu⁶⁵, X. Yuan^{36,w}, O. Yushchenko³⁷, K.A. Zarebski⁴⁷, M. Zavertyaev^{11,c}, L. Zhang³, Y. Zhang⁷, Y. Zhang⁶³, A. Zhelezov¹², Y. Zheng⁶³, X. Zhu³, V. Zhukov³³, S. Zucchelli¹⁵

¹ Centro Brasileiro de Pesquisas Físicas (CBPF), Rio de Janeiro, Brazil

² Universidade Federal do Rio de Janeiro (UFRJ), Rio de Janeiro, Brazil

³ Center for High Energy Physics, Tsinghua University, Beijing, China

⁴ LAPP, Université Savoie Mont-Blanc, CNRS/IN2P3, Annecy-Le-Vieux, France

⁵ Clermont Université, Université Blaise Pascal, CNRS/IN2P3, LPC, Clermont-Ferrand, France

⁶ CPPM, Aix-Marseille Université, CNRS/IN2P3, Marseille, France

⁷ LAL, Université Paris-Sud, CNRS/IN2P3, Orsay, France

⁸ LPNHE, Université Pierre et Marie Curie, Université Paris Diderot, CNRS/IN2P3, Paris, France

⁹ I. Physikalisches Institut, RWTH Aachen University, Aachen, Germany

¹⁰ Fakultät Physik, Technische Universität Dortmund, Dortmund, Germany

¹¹ Max-Planck-Institut für Kernphysik (MPIK), Heidelberg, Germany

¹² Physikalisches Institut, Ruprecht-Karls-Universität Heidelberg, Heidelberg, Germany

¹³ School of Physics, University College Dublin, Dublin, Ireland

¹⁴ Sezione INFN di Bari, Bari, Italy

¹⁵ Sezione INFN di Bologna, Bologna, Italy

¹⁶ Sezione INFN di Cagliari, Cagliari, Italy

- ¹⁷ *Sezione INFN di Ferrara, Ferrara, Italy*
- ¹⁸ *Sezione INFN di Firenze, Firenze, Italy*
- ¹⁹ *Laboratori Nazionali dell'INFN di Frascati, Frascati, Italy*
- ²⁰ *Sezione INFN di Genova, Genova, Italy*
- ²¹ *Sezione INFN di Milano Bicocca, Milano, Italy*
- ²² *Sezione INFN di Milano, Milano, Italy*
- ²³ *Sezione INFN di Padova, Padova, Italy*
- ²⁴ *Sezione INFN di Pisa, Pisa, Italy*
- ²⁵ *Sezione INFN di Roma Tor Vergata, Roma, Italy*
- ²⁶ *Sezione INFN di Roma La Sapienza, Roma, Italy*
- ²⁷ *Henryk Niewodniczanski Institute of Nuclear Physics Polish Academy of Sciences, Kraków, Poland*
- ²⁸ *AGH — University of Science and Technology, Faculty of Physics and Applied Computer Science, Kraków, Poland*
- ²⁹ *National Center for Nuclear Research (NCBJ), Warsaw, Poland*
- ³⁰ *Horia Hulubei National Institute of Physics and Nuclear Engineering, Bucharest-Magurele, Romania*
- ³¹ *Petersburg Nuclear Physics Institute (PNPI), Gatchina, Russia*
- ³² *Institute of Theoretical and Experimental Physics (ITEP), Moscow, Russia*
- ³³ *Institute of Nuclear Physics, Moscow State University (SINP MSU), Moscow, Russia*
- ³⁴ *Institute for Nuclear Research of the Russian Academy of Sciences (INR RAN), Moscow, Russia*
- ³⁵ *Yandex School of Data Analysis, Moscow, Russia*
- ³⁶ *Budker Institute of Nuclear Physics (SB RAS), Novosibirsk, Russia*
- ³⁷ *Institute for High Energy Physics (IHEP), Protvino, Russia*
- ³⁸ *ICCUB, Universitat de Barcelona, Barcelona, Spain*
- ³⁹ *Universidad de Santiago de Compostela, Santiago de Compostela, Spain*
- ⁴⁰ *European Organization for Nuclear Research (CERN), Geneva, Switzerland*
- ⁴¹ *Institute of Physics, Ecole Polytechnique Fédérale de Lausanne (EPFL), Lausanne, Switzerland*
- ⁴² *Physik-Institut, Universität Zürich, Zürich, Switzerland*
- ⁴³ *Nikhef National Institute for Subatomic Physics, Amsterdam, The Netherlands*
- ⁴⁴ *Nikhef National Institute for Subatomic Physics and VU University Amsterdam, Amsterdam, The Netherlands*
- ⁴⁵ *NSC Kharkiv Institute of Physics and Technology (NSC KIPT), Kharkiv, Ukraine*
- ⁴⁶ *Institute for Nuclear Research of the National Academy of Sciences (KINR), Kyiv, Ukraine*
- ⁴⁷ *University of Birmingham, Birmingham, United Kingdom*
- ⁴⁸ *H.H. Wills Physics Laboratory, University of Bristol, Bristol, United Kingdom*
- ⁴⁹ *Cavendish Laboratory, University of Cambridge, Cambridge, United Kingdom*
- ⁵⁰ *Department of Physics, University of Warwick, Coventry, United Kingdom*
- ⁵¹ *STFC Rutherford Appleton Laboratory, Didcot, United Kingdom*
- ⁵² *School of Physics and Astronomy, University of Edinburgh, Edinburgh, United Kingdom*
- ⁵³ *School of Physics and Astronomy, University of Glasgow, Glasgow, United Kingdom*
- ⁵⁴ *Oliver Lodge Laboratory, University of Liverpool, Liverpool, United Kingdom*
- ⁵⁵ *Imperial College London, London, United Kingdom*
- ⁵⁶ *School of Physics and Astronomy, University of Manchester, Manchester, United Kingdom*
- ⁵⁷ *Department of Physics, University of Oxford, Oxford, United Kingdom*
- ⁵⁸ *Massachusetts Institute of Technology, Cambridge, MA, United States*
- ⁵⁹ *University of Cincinnati, Cincinnati, OH, United States*
- ⁶⁰ *University of Maryland, College Park, MD, United States*
- ⁶¹ *Syracuse University, Syracuse, NY, United States*
- ⁶² *Pontifícia Universidade Católica do Rio de Janeiro (PUC-Rio), Rio de Janeiro, Brazil, associated to²*
- ⁶³ *University of Chinese Academy of Sciences, Beijing, China, associated to³*
- ⁶⁴ *School of Physics and Technology, Wuhan University, Wuhan, China, associated to³*

- ⁶⁵ *Institute of Particle Physics, Central China Normal University, Wuhan, Hubei, China, associated to*³
- ⁶⁶ *Departamento de Fisica , Universidad Nacional de Colombia, Bogota, Colombia, associated to*⁸
- ⁶⁷ *Institut für Physik, Universität Rostock, Rostock, Germany, associated to*¹²
- ⁶⁸ *National Research Centre Kurchatov Institute, Moscow, Russia, associated to*³²
- ⁶⁹ *Instituto de Fisica Corpuscular (IFIC), Universitat de Valencia-CSIC, Valencia, Spain, associated to*³⁸
- ⁷⁰ *Van Swinderen Institute, University of Groningen, Groningen, The Netherlands, associated to*⁴³
- ^a *Universidade Federal do Triângulo Mineiro (UFTM), Uberaba-MG, Brazil*
- ^b *Laboratoire Leprince-Ringuet, Palaiseau, France*
- ^c *P.N. Lebedev Physical Institute, Russian Academy of Science (LPI RAS), Moscow, Russia*
- ^d *Università di Bari, Bari, Italy*
- ^e *Università di Bologna, Bologna, Italy*
- ^f *Università di Cagliari, Cagliari, Italy*
- ^g *Università di Ferrara, Ferrara, Italy*
- ^h *Università di Genova, Genova, Italy*
- ⁱ *Università di Milano Bicocca, Milano, Italy*
- ^j *Università di Roma Tor Vergata, Roma, Italy*
- ^k *Università di Roma La Sapienza, Roma, Italy*
- ^l *AGH — University of Science and Technology, Faculty of Computer Science, Electronics and Telecommunications, Kraków, Poland*
- ^m *LIFAELS, La Salle, Universitat Ramon Llull, Barcelona, Spain*
- ⁿ *Hanoi University of Science, Hanoi, Viet Nam*
- ^o *Università di Padova, Padova, Italy*
- ^p *Università di Pisa, Pisa, Italy*
- ^q *Università degli Studi di Milano, Milano, Italy*
- ^r *Università di Urbino, Urbino, Italy*
- ^s *Università della Basilicata, Potenza, Italy*
- ^t *Scuola Normale Superiore, Pisa, Italy*
- ^u *Università di Modena e Reggio Emilia, Modena, Italy*
- ^v *Iligan Institute of Technology (IIT), Iligan, Philippines*
- ^w *Novosibirsk State University, Novosibirsk, Russia* [†]Deceased